International Journal of Research in Medical Sciences
*Gloi AM et al. Int J Res Med Sci. 2023 Sep;11(9):3206-3211*
www.msjonline.org
pISSN 2320-6071 | eISSN 2320-6012

DOI: https://dx.doi.org/10.18203/2320-6012.ijrms20232769

**Original Research Article**

# Forecasting machine performance check output using Holt-Winters approach

**Aime M. Gloi*, Vladimir Stankovich, Benjamin Rodriguez, Stanley Mayas**

Department of Radiation Oncology. Genesiscare, Modesto, California, USA

**Received:** 12 July 2023
**Revised:** 03 August 2023
**Accepted:** 04 August 2023

***Correspondence:**
Aime M. Gloi,
E-mail: agloi7288@gmail.com



## ABSTRACT

**Background:** Machine Performance Check (MPC) is an automated TrueBeam quality control (QC) tool used to verify beam output, isocenter, and uniformity. The aim of this study was to build an MPC output variation time series modeled on the Holt-Winters method over thirty days.
**Methods:** After AAPM TG-51 and baseline data were established for the Edge TrueBeam, daily MPC output data were gathered and analyzed through a Holt-Winters (additive and multiplicative) method. The model's performance was assessed via three standard error measures: the mean squared error (MSE), the mean absolute percentage error (MAPE), and the mean absolute deviation (MAE). The aim was achieved using a nonlinear multistart solver on the Excel platform.
**Results:** The results showed that MPC output variation forecasting is energy and model dependent. Both additive and multiplicative Holt-Winters methods were suitable for the analysis. The performance metrics MSE, MAPE, and MAD were found to be well within acceptable limits.
**Conclusions:** A Holt-Winters model was able to accurately forecast the MPC output variation.

**Keywords:** Machine performance check, Holt-Winters additive method, Multiplicative method

## INTRODUCTION

The main aim of radiation therapy is to deliver a dose to a target volume while protecting the surrounding organs. To ensure proper and accurate dose distribution, quality assurance (QA) of a linear accelerator (linac) is performed daily, weekly, monthly, and annually to a clinically acceptable commissioned data tolerance based on the relevant guidelines.[1-3]

Traditionally, linac output QA tests are conducted on the Daily QA3 (QA3) system (Sun Nuclear Corporation; Melbourne, USA) before any patient treatment. Recently, a novel system, the machine performance check (MPC), derived from the TrueBeam Edge 2.0 platform (Varian Medical Systems, Palo Alto, CA, USA), has been suggested. It relies on a fully integrated and automated imaging system that includes an electronic portal imaging device (EPID), kilovoltage (kV), megavoltage (MV), and an on-board imager (OBI). The MPC-EPID-based system, a 2D detector array ushered in by Baily et al can perform daily output checks.[4] First intended for patient position verification, it has emerged as a dosimetric and now as a linac output verification.[5,6] In this study, the variation in daily output in terms of photon and electron energies was monitored over a month to follow trends and patterns in the measurement. Hosain et al suggested that the linac output variation may be because of an environmental and seasonal deviation, causing cyclical changes that affect electronic response.[7] Other have stated that the uncorrected output could increase or decrease sometimes and could be possibily attributed to the disparity in the monitor chamber design differences.[8,9] Equally important, the representation of the level (α), trend (β), and seasonality (γ), in the output data is triggered by infrequent output modifications and tunings made to the linac, thus creating gaps in the measured data caused by service maintenance events. Therefore, forecasting is vital and warranted for decision-making and strategic planning. Forecasting involves three main stages that include short, medium, and long-term strategies dependent on the planning quality assurance (QA) schedule. In this report, the Holt-Winters (HW) method with triple exponential smoothing was used to reduce irregularities in the time series data.[10] Usually, historical data are used as input to make informed estimates that are predictive in terms of determining the direction of future trends. As a result, preventive maintenance could start to improve efficiency and reduce linac downtime. To the best of our knowledge, this is the first comparative report based on MPC output variation modeled by HW.

## METHODS

A research output measurements study from an Edge TrueBeam (Varian Medical Systems, Palo Alto) linac were carried out based on clinically available photon (6 and 10 MV, 6 and 10 free flattening filter (FFF) and electron (6, 9, 12, 15 MeV) energies. First, the linac was calibrated annually using the AAPM TG51 protocol.[11] Then, MPC baseline data was obtained. Finally, MPC's daily output was acquired and recorded over thirty days from May to June 2022 at Genesis Care Clinic.

### *MPC variation forecast*

MPC output variation forecasts were conducted using HW time series. It is a combination of triple exponential smoothing that includes level (α), trend (β), and seasonality (γ), and is characterized by the following equations:

### *Overall smoothing*

$$S_t = \alpha \frac{y_t}{I_t - L} + (1-\alpha)(S_{t-1} + b_{t-1}) \qquad \text{..........1}$$

### *Smoothing by trend*

$$b_t = \beta(S_t - S_{t-1}) + (1-\beta)b_{t-1} \qquad \text{..........2}$$

### *Smoothing by seasonality*

$$I_t = \gamma \frac{y_t}{S_t} + (1-\gamma)I_{t-L} \qquad \text{..........3}$$

The total forecast is given by the equations;

$$F_{t+m} = (S_t + mb_t)I_{t-L+m} \text{.........4}$$

Which is multiplicative and by;

$$F_{t+m} = (S_t + mb_t) + I_{t-L+m} \qquad \text{..........5}$$

Which is additive.

Where 0 < α < 1; 0 < β < 1; 0 < γ < 1, and α represents the level smoothing factor, β constitutes the trend-smoothing factor and γ serves as the seasonality smoothing factor. y and S are the actual and smoothed observations, where b is the trend factor, I is the seasonal index, F is the forecast, m are steps ahead, L is the cycle length, and t is the period. The method is based on five equations that calculate the value of the sequence in the past (level), the future tendency (trend), and a seasonal term (seasonality), which allows for the development of repetitive patterns. Finally, equations mentioned above compute the weighted sum of the previous terms as a forecast. The general architecture of this study is shown in (Figure 1). The (Table 1) summarizes both HW additive (HWA) and multiplicative (HWM) approaches.

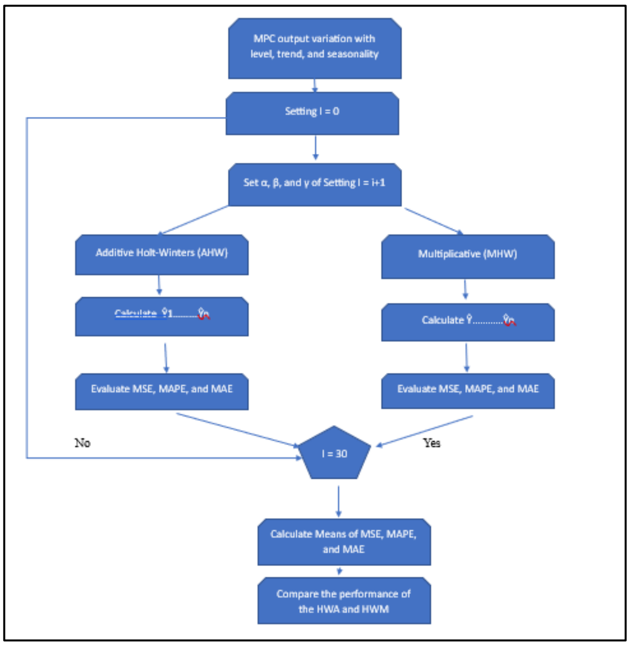


**Figure 1: Flow chart of the MPC output variation forecast simulation.**

### *Optimization*

Goodness-of-fit is the measure of the accuracy of the predicted model compared to actual values. A classic approach is based on the closeness between the predicted and actual values. Three measurement criteria were employed in this study: the mean squared error (MSE), the mean absolute percentage error (MAPE), and the mean absolute deviation (MAE). For all three metrics, the smaller the value, the better the predicted accuracy.

### *Mean squared error*

The MSE is a measure of the dispersion of forecast errors. The smaller the value of the MSE, the more stable the model.

$$MSE = \frac{1}{n}\sum_{i=1}^{n}(pred_i - actual_i)^2 \text{ ........6}$$

***Mean absolute percentage error***

The MAPE is an error measurement that does not emphasize large errors. The MAPE is given by:

$$MAPE = \frac{1}{n}\sum_{i=1}^{n}\left|\frac{actual_i - pred_i}{actual_i}\right| \text{ ........7}$$

***Mean absolute error***

The MAE can be described as the average of the absolute error value without regard to whether the error was overestimated or underestimated.

$$MAE = \frac{\sum_{i=1}^{n}(pred_i - actual_i)}{n} \text{ ........8}$$

An Excel-based nonlinear optimizer solver, namely a generalized reduced gradient (GRG) optimization, was used to identify the values of the smoothing constants by minimizing MSE and deducing optimized (α, β, y) factors. MSE, MAPE, and MAE were determined to assess the model fit.

**Table 1: Comparative equations for the multiplicative and additive Holt-Winters models.**

| Parameters | Additive Holt-Winters | Multiplicative Holt-Winters |
|---|---|---|
| **Level** | $S_t = \alpha \frac{y_t}{I_t - L} + (1-\alpha)(S_{t-1} + b_{t-1})$ | $S_t = \alpha \frac{y_t}{I_t - L} + (1-\alpha)(S_{t-1} + b_{t-1})$ |
| **Trend** | $b_t = \beta(S_t - S_{t-1}) + (1-\beta)b_{t-1}$ | $b_t = \beta(S_t - S_{t-1}) + (1-\beta)b_{t-1}$ |
| **Seasonality** | $I_t = \gamma \frac{y_t}{S_t} + (1-\gamma)I_{t-L}$ | $I_t = \gamma \frac{y_t}{S_t} + (1-\gamma)I_{t-L}$ |
| **Forecast** | $F_{t+m} = (S_t + mb_t) + I_{t-L+m}$ | $F_{t+m} = (S_t + mb_t)I_{t-L+m}$ |

**Table 2: Performance quantities of the HW model additive.**

| Parameters | 6MV | 6FFF | 10MV | 10FFF | 6 MeV | 9 MeV | 12 MeV | 15 MeV |
|---|---|---|---|---|---|---|---|---|
| **α** | 0.0426 | 0.4764 | 0.6314 | 0.4633 | 0.5910 | 0.6277 | 0.5647 | 0.5970 |
| **β** | 1 | 0 | 0.0255 | 0.0163 | 0.0411 | 0.0588 | 0 | 0.0877 |
| **γ** | 0.4408 | 0.6345 | 0.7614 | 0.5172 | 1 | 1 | 1 | 0.9967 |
| **MSE** | 0.0244 | 0.0094 | 0.0091 | 0.0087 | 0.0920 | 0.0325 | 0.0138 | 0.0164 |
| **MAE** | 0.1360 | 0.0944 | 0.0092 | 0.0942 | 0.2591 | 0.1540 | 0.0917 | 0.1065 |
| **MAPE** | 1.5775 | 1.5869 | 0.5321 | 0.5368 | 2.0016 | 1.0681 | 11.4929 | 1.1461 |

**Table 3: Performance quantities of the HW model multiplicative.**

| Parameters | 6MV | 6FFF | 10MV | 10 FFF | 6 MeV | 9 MeV | 12 MeV | 15 MeV |
|---|---|---|---|---|---|---|---|---|
| **α** | 0.1456 | 0.2832 | 0.0066 | 0.1339 | 0.0283 | 0.0520 | 0.020569 | 0.2410 |
| **β** | 0.1713 | 0.5895 | 0.0243 | 0.0557 | 0.3497 | 0.0854 | 0 | 0.5746 |
| **γ** | 0.0407 | 0.3066 | 0.3927 | 0.5764 | 0.0018 | 0.2709 | 0.8953 | 0.5898 |
| **MSE** | 0.0195 | 0.0099 | 0.0142 | 0.0114 | 0.0669 | 0.0434 | 0.0214 | 0.0177 |
| **MAE** | 0.1084 | 0.0801 | 0.0941 | 0.0817 | 0.2123 | 0.1738 | 0.1189 | 0.0987 |
| **MAPE** | 0.6922 | 1.2452 | 0.6038 | 0.4540 | 1.1421 | 1.0017 | 9.5019 | 0.9277 |

## RESULTS

The HW forecasting method was achieved by minimizing the MSE (prediction error) using GRG with initial smoothing parameters ($\alpha_0$, $\beta_0$, $\gamma_0$). Three smoothing parameters (α, β, γ) were attained based on better convergence between observed and estimated MPC output data. Tables 2 and 3 show the derived smoothing parameter values and the performance metrics MSE, MAPE, and MAE for seasonal HWA and HWM. Values close to zero for the smoothing parameters suggest that little weight is placed on the most recent observations when predicting future values. In contrast, values closer to one suggest that much more weight is associated with observations in the far distant past when acquiring forecast values. However, the estimated value of zero for β shows that slope b of the trend component of the seasonal HWA is not revised over the time series but is set equal to its initial value. In this study, both models produced relatively small MSE errors, implying that they could be used as a better metric than MAPE or MAE. Yet HWM had a lower MAPE than HWA. A benchmark of less than 10% for

MAPE was deemed for highly accurate models [12]. Both models had a MAPE of less than 10, showing high performance. Figure 2 illustrates the performance metrics of MSE, MAPE, and MAE results. They revealed average MSE values of 0.0257±0.02655 and 0.0255±0.0184 for HWA and HWM seasonality, respectively.

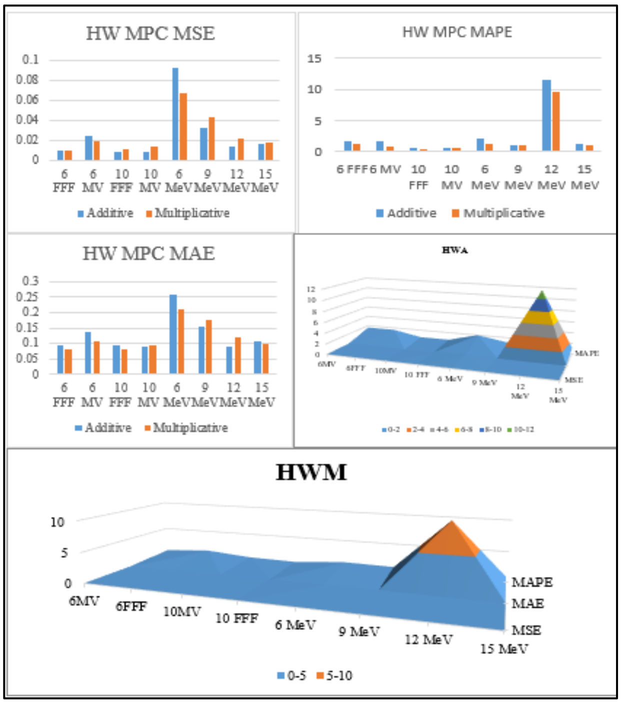


**Figure 2: MSE, MAPE, and MAE values for MPC datasets output variation using the additive and multiplicative Holt- Winters methods. Symbol A and M denote additive and multiplicative, respectively.**

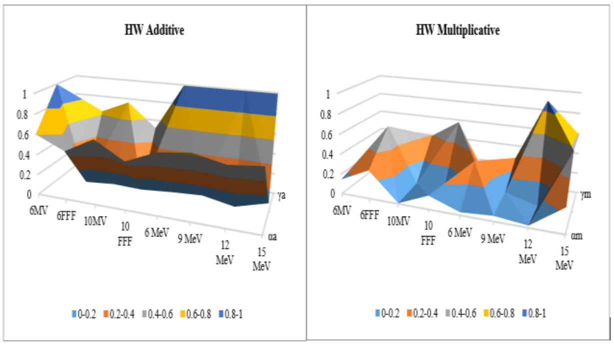


**Figure 3: HW Smooth parameters (α, β, γ) derived to minimize MSE: a, m denotes additive and multiplicative, respectively.**

The MAPE values were estimated as 2.4927±3.4354 and 1.9460±2.86669 for HWA and HWM seasonality, respectively. Also, the MAE values were calculated as 0.1181±0.0710 and 0.1210±0.04739 for HWA and HWM seasonality, respectively. In this study, the MSE for MPC output predictions is less than or equal to 0.05 for all energies. A lower MSE corresponds to a predictive model that better correlates with the actual variation in the MPC output. In addition, optimized values of the smoothing parameters (α, β, γ) were found by converging MSE to its lowest possible value for each energy. The final convergence behavior for all performance metrics MSE, MAPE, and MAE for each model is displayed in Figure 2 for HWA and HWM, respectively.

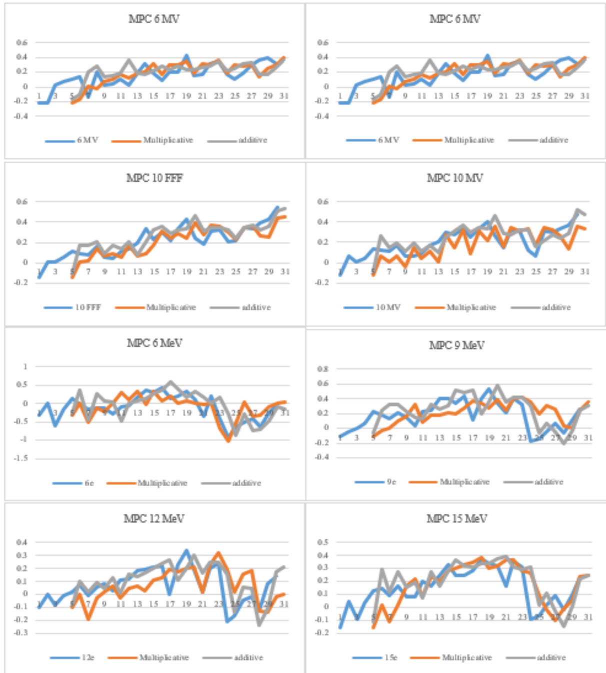


**Figure 4: Comparison between HW multiplicative and additive method in level, trend, and seasonality.**

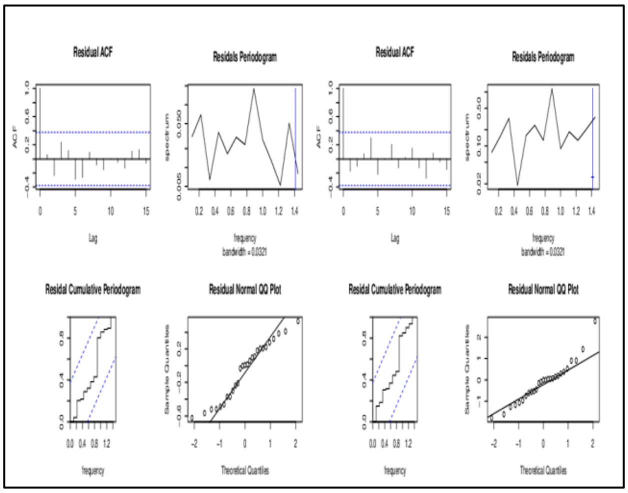


**Figure 5: Residual diagnostics of additive and multiplicative HW Smoothing for MPC output variation with 6 MeV.**

Further, the influence of the smoothing parameters (α, β, γ) on the objective function MSE was assessed and displayed in Figure 3 for HWA and HWM, respectively. These parameters characterize the underlying dynamics of the time series. Figure 4 presents the fitted seasonal factor, level, and trend for the MPC output variations between observed and forecasted values via Holt-Winters multiplicative and additive model decomposition for all energies.

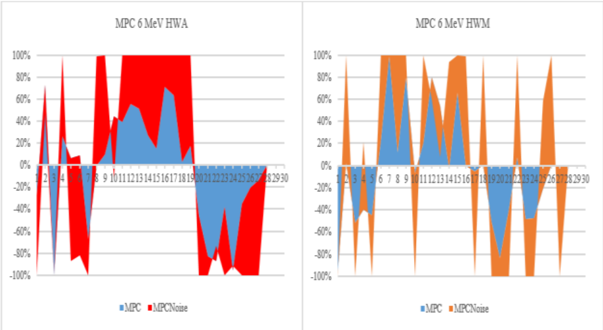


**Figure 6: Additive HW and multiplicative HW Gaussian white noise with 6 MeV.**

For completeness, an additional investigation was conducted on one energy (6 MeV). While most of the results from error measurements were relatively small, a test of the residuals was performed for white noise validation without any patterns. Consequently, the autocorrelation function (ACF) was computed and examined to verify that all residuals gravitated around zero. Figure 5 shows the MPC output variation residual for 6 MeV. Based on the ACF and periodogram residuals plots, the spikes are within the suggested limits, meaning none is significant and thus not autocorrelated. Afterwards, the plots corroborate that the variance is constant, and the mean of the residuals is zero. Hence, the residual data closely follows a normal distribution. As a result, the HW model evaluates the seasonal effects. Besides, a normal QQ plot also shows that the residuals were normally distributed and that all patterns lie within the 95% confidence interval. Again, this is an indicator of the significance threshold, suggesting that anything within the dotted area is statistically close to zero and anything outside is statistically non-zero. Additionally, the model robustness was tested using Gaussian white noise with different intensities for both HWA and HWM. The randomly generated Gaussian white noise is illustrated in Figure 6 with the corresponding noise intensity. The inherent robustness is evaluated via the effect of the noise intensity over the accuracy of the model, measured by the coefficient of determination $R^2$. Low variance in $R^2$ shows high robustness, whereas high variance denotes low robustness. In fact, the correlation and determination coefficients were $R^2$ (0.339, 0.282) and (0.115, 0.076) for both HWA and HWM, respectively.

## DISCUSSION

The HW model was applied to the MPC output dataset over thirty days with specifications for the level, trend, and seasonal components, which were instrumental in the forecasting procedure. The analysis showed that both HW models were suitable for MPC output variation forecasting since the value of MSE was smaller for all energies compared to the other performance metrics, MAPE and MAE. It follows from the report that the smoothing parameters (α, β, γ) are energy- and HW-specific. The need to select the model's initial values is one of its main disadvantages. These parameters affect the level, trend, and seasonality.

Moreover, MPC output forecast modeling through the HW method for different energies is subject to the inherent long-term pixel stability of the EPID panels. They exhibit a variation between 0.29% and 0.6% per pixel, and 99% of all pixels show a deviation of less than 1%, as noted by several investigators.[13,14] Further, EPID panels are contingent on maintenance and recalibration procedures, which are the most likely sources of unexpected systematic changes in MPC output values, as reported by Barnes et al.[15] Other events may include the EPID ghosting effect, which usually depicts the modification of detector response due to previous irradiation. As a result, the magnitude of ghosting will depend on the number of monitor units delivered as well as the time interval used between the two radiation fields.

Therefore, it will change the sensitivity of the detector and affect the image gain correction to the pixel sensitivity distribution.[16] Several authors have also reported on the flux of the dose-response reproducibility of the EPID system, characterized by 1.0% variability from the nominal output, and have suggested that the beam flatness is a major contributor to the MPC output deviation.[17-20] They attribute this drift in the MPC response to the continuing fading in panel sensitivity. These events will alter MPC output and hence the input data for the forecast model. Future works will involve the use of a neural network (NN) model that will be used to house the correlation between two nonlinear variables (actual and forecasted). Also, various moving average models such as autoregressive moving average (ARMA), autoregressive integrated moving average (ARIMA), and autoregressive integrated moving average-neural network (ARIMA-NN) are of greatest interest and could be used for comparison. Finally, Theil's U statistics will be used to verify the accuracy test of the model and will allow us to compare the predicted results to the actual model results with minimal historical data.

## CONCLUSION

The aim of the study was to forecast MPC output and identify patterns via Holt-Winters smoothing. The study showed that HW, both additive and multiplicative, is adequate for MPC output modeling. Performance metrics such as RMSE, MAPE, and MAE could assess HW goodness of fit. The model robustness could be evaluated using the residuals through ACF and the cumulative periodogram.

*Funding: No funding sources*
*Conflict of interest: None declared*
*Ethical approval: The study was approved by the Institutional Ethics Committee*

## REFERENCES


1. Kutcher GJ, Coia L, Gillin M, Hanson WF, Leibel S, Morton RJ, et al. Comprehensive QA for Radiation Oncology Report of AAPM Radiation-Therapy Committee Task-Group-40. Med Phys. 1994;21(4): 581-618.
2. Morton RJ. Quality Assurance for Medical Accelerators. Med Phys. 2011;38(6):361-9.
3. Bissonnette J, Balter P, Dong Lei. Quality assurance for image-guided radiation therapy utilizing CT-based technologies: a report of the AAPM TG-179. Med Phys. 2012; 39(4):1946-63.
4. Baily NA, Horn RA, Kampp TD. Fluoroscopic visualization of megavoltage therapeutic x ray beams. Int J Radiat Oncol. 1980;6:935-9.
5. Fuangrod T, Rowshanfarzad P, Greer PB. A cine-EPID based method for jaw detection and quality assurance for tracking jaw in IMRT/VMAT treatments. Phys Med. 2015;31:16-24.
6. Ding A, Xing L, Han B. Development of an accurate EPID-based output measurement and dosimetric verification tool for electron beam therapy. Med Phys. 2015;42:4190-8.
7. Hossain M. Output trends, characteristics, and measurements of three megavoltage radiotherapy linear accelerators. J App Clin Med Physics. 2014;15: 32-8.
8. Luketina IA, Gregg L. Linear accelerator output variability. Australas Phys Eng Sci Med. 2004;27(3): 155-9
9. Kapanen M, Tenhunen M, Hamalainen T, Sipila P, Parkkinen R, Jarvinen H. Analysis of quality control data of eight modern radiotherapy linear accelerators: the short- and long-term behaviors of the outputs and the reproducibility of quality control measurements. Phys Med Biol. 2006;51(14):3581-92
10. Holt CC. Forecasting trends and seasonal by exponentially weighted moving averages. ONR Memo. 1957.
11. Almond PR, Biggs PJ, Coursey BM, Hanson WF, Huq MS, Nath R, et al. AAPM's TG-51 protocol for clinical reference dosimetry of high-energy photon and electron beams Med Phys 1999;26(9):1847-70.
12. Lewis CD. Demand forecasting and inventory control. New York: John Wiley and Sons, Inc; 1997.
13. Barnes MP, Greer PB. Evaluation of the TrueBeam machine performance check (MPC) beam constancy checks for flattened and flattening filter-free (FFF) photon beams. J Appl Clin Med Phys. 2017;18:139-50.
14. Barnes MP, Greer PB. Evaluation of the Truebeam machine performance check (MPC) geometric checks for daily IGRT geometric accuracy quality assurance. J Appl Clin Med Phys. 2017;18:200-206.
15. Barnes MP, Greer PB. Evaluation of the Truebeam machine performance check (MPC): mechanical and collimation checks. J Appl Clin Med Phys. 2017;18: 56-66.
16. McDermott LC, Louwe RJW, Sonke JJ, van Herk MB. Dose-response and ghosting effects of an amorphous silicon electronic portal imaging device. Med Phys. 2004;31(2):285-95.
17. Barnes MP, Pomare D, Menk FW, Moraro B, Greer PB. Evaluation of the Truebeam machine performance check (MPC): OBI X-ray tube alignment procedure. J Appl Clin Med Phys. 2018;19:68-78.
18. Gao S, Balter PA, Rose M, Simon WE. Measurement of changes in linear accelerator photon energy through flatness variation using an ion chamber array. Med Phys. 2013;40(4):143-9.
19. Goodall S, Harding N, Simpson J, Alexander L, Morgan S. Clinical implementation of photon beam flatness measurements to verify beam quality. J Appl Clin Med Phys. 2015;16(6):340-5.
20. Hossain M, Rhoades J. On beam quality and flatness of radiotherapy megavoltage photon beams. Australas Phys Eng S. 2016;39(1):135-45.


**Cite this article as:** Gloi AM, Stankovich V, Rodriguez B, Mayas S. Forecasting machine performance check output using Holt-Winters approach. Int J Res Med Sci 2023;11:3206-11.